https://dx.doi.org/10.21577/0103-5053.20230091

J. Braz. Chem. Soc., Vol. 34, No. 11, 1631-1640, 2023

Article

Evaluation of Extraction Parameters for the Analysis of Lipid Classes in Plants

Taynara S. Matos,[a] Mariana S. Marques,[a] Cleber J. N. Chaves,[b] Flávia S. Zandonadi,[a] Clarisse Palma-Silva[b] and Alessandra Sussulini[*,a,c]*

[a]*Laboratório de Bioanalítica e Ciências Ômicas Integradas (LaBIOmics), Departamento de Química Analítica, Instituto de Química, Universidade Estadual de Campinas (UNICAMP), 13083-862 Campinas-SP, Brazil*

[b]*Laboratório de Ecologia Molecular e Genômica Evolutiva de Plantas, Instituto de Biologia, Universidade Estadual de Campinas (UNICAMP), 13083-861 Campinas-SP, Brazil*

[c]*Instituto Nacional de Ciência e Tecnologia em Bioanalítica (INCTBio), Universidade Estadual de Campinas (UNICAMP), 13083-862 Campinas-SP, Brazil*

The aim of this study was to preliminary evaluate the lipid profile alterations on *Pitcairnia flammea* leaves based on variations in solvent proportion and ultrasonic ice bath extraction time, followed by a lipid class-enriched analysis employing chemometric techniques. Ultra-high performance liquid chromatography coupled to electrospray ionization mass spectrometry (UHPLC-ESI-MS) was used to acquire raw data and MS-DIAL and MetaboAnalyst platforms were used to perform data preprocessing and statistical analysis. The statistical analysis of UHPLC-ESI-MS data in both ionization modes enabled the visualization of a trend distribution based on extraction time. Furthermore, we were able to establish that the solvent proportion had a greater impact on group separation in data samples extracted for 30 min *versus* 10 and 20 min. Moreover, diacylglycerol or/and lysophosphatidylcholine are lipid subclasses that can be favored depending on the extraction time in the mass spectrometry analyses using positive electrospray ionization mode.

Keywords: sample preparation, extraction techniques, untargeted lipidomics, UHPLC-ESI-MS, plant lipidomics

Introduction

Metabolomics is defined as the study of low molecular mass compounds that cooperate in biological processes and, in many cases, act as key regulators in many metabolic activities in a variety of species.[1] Lipidomics, a term used to describe an approach that focuses more specifically on lipid analysis,[2] has become an important branch of metabolomics and brought new information on various plant metabolic processes.[3]

Lipids are small hydrophobic or amphiphilic molecules, that also modulate a wide range of biological functions in cells, tissues, organs, and organisms.[4] They act in energy storage, chemical transport, vitamin absorption, and hormone production. In plants, non-canonical biological processes cell signaling,[5] biotic and abiotic stress control tolerance,[6] and the use of plant-derived membrane-enclosed extracellular vesicles (P-EVs) for cell-to-cell communication,[7] are mediated by lipids. In an evaluation of *Arabidopsis* leaf extracellular vesicles, for example, 23 lipid classes were identified, using liquid chromatography coupled to mass spectrometry-based techniques, but revealed that these structures are composed of nearly pure glycosylinositolphosphoceramides, providing valuable information on the biogenesis of P-EVs.[5]

Mass spectrometry is the most widely used analytical technique for lipidomics, due to its high sensitivity, coupled with chromatographic techniques, especially liquid chromatography.[2] This combination allows an ion suppression reduction, and increases the selectivity, important advantages on complex matrices analyses.[8] The use of reversed-phase liquid chromatography as separation mode has improved this association, allowing a broad range analysis of molecular structures like phospholipids and

*e-mail: sussulini@unicamp.br
Dedicated to our dearest Prof. Carol Collins, the "mother" of chromatography in Brazil.
Editor handled this article: Andréa R. Chaves (Associate)

short-chain fatty acids.[9] These characteristics are crucial to untargeted phytocompounds analysis. Another important procedure in metabolomics/lipidomics is biological sample handling, which is important to maintain the reliability and representativity of the material metabolome.[10] To fully make use of the advantages of these analytical techniques, it is necessary to employ sample preparation methods that guarantee the removal of interferents and help to increase analyte concentration.

Sample preparation is, therefore, a crucial step to select the class of metabolites to be analyzed, reduce sample complexity, and define the parameters within the selected analytical technique.[11] This step is essential to guarantee cell membrane lysis, and biological processes interruption since they control some aspects of reducing metabolites and lipids turnover, especially those highly oxidation and degradation susceptibility. These processes can be done with the use of solvents (e.g., methanol, acetonitrile) or freeze-thaw cycles. In addition to a reproducible and simple method of preparation, quality control procedures can monitor the stability of analytical equipment, allowing higher quality data to be obtained.[9]

Plant lipidomic studies have been employing different extraction methods including different solvents and their proportion.[3] Recently, Sun *et al.*[12] compared Folch and Bligh & Dyer extraction to analyze lipids during the banana ripening. In their study, it was found that the second method presented an extraction efficiency enhancement of total lipid analysis compared to the first procedure. However, most of these studies are based on sample preparation and extraction techniques for biological fluids, mostly blood serum and plasma.[5]

Therefore, it is unconditionally important the sample preparation procedures improvement and new approaches development, in order to optimize the information quality on sample molecular identification. Under this context, this work provides a preliminary description on leaf sample extraction parameters, focusing on how solvent proportions and time of extraction are impacting the whole bromeliad lipidome, and also which lipid classes are most affected by time and solvent changes. The bromeliad leaves were used as a case study. For that, our results are based on untargeted ultra-high performance liquid chromatography coupled to electrospray ionization mass spectrometry (UHPLC-ESI-MS) analysis and bioinformatic tools.

Experimental

Chemicals

Methanol (MeOH, HPLC grade, 99.9% purity), and acetonitrile were acquired from Millipore (Billerica, USA). Methyl *tert*-butyl ether (MTBE, HPLC grade, 99.9% purity), ammonium acetate (NH_4Ac, 99.0% purity), and 2-propanol (99.9% purity) were purchased from Sigma Chemicals (St. Louis, USA). Type 1 (ultrapure) water was obtained in a Milli-Q system (Millipore, Bedford, USA).

Sample storage conditions

We collected leaf samples of individuals of *Pitcairnia flammea*, an endemic species from the Atlantic Rainforest. Distinct elevations cultivated at the Institute of Biology (UNICAMP, Brazil) were harvested and immediately frozen in liquid nitrogen (–195.8 ºC) in order to quench enzymatic activities, followed the –80 ºC storage in a 50 mL conic tube, until sample preparation. For sample preparation, the leaves were macerated to fine powder using a mortar and pestle in liquid nitrogen condition. Access to genetic heritage was registered at the National System of Genetic Resource Management and Associated Traditional Knowledge (SisGen) under code number A3C2E73.

Sample extraction

The processes used in this study were based on the method developed by Hummel *et al.*[13] for plant lipid analysis using UHPLC-ESI-MS. In this method, the sample is separated into 3 phases: organic, aqueous and protein. It is noteworthy that the lower phase can also have other solid matter besides proteins, as fibers. 10 mL of solvent mixture were prepared in 3 different proportions (1:2, 1:3 or 1:4 (v/v)), pre-cooled at 20 ºC in MeOH and MTBE.

In 2 mL tubes, 50 mg of macerated sample were added and 1 mL of the solvent mixture. The samples were incubated for 5 min under agitation at 500 rpm at 4 ºC in a microtube shaking incubator (AccuTherm, Labnet International Inc., Corning, USA), followed by ultra sonication in an ultrasonic bath (5800, Branson Ultrasonics Corporation, Danbury, USA) in ice-cold bath in different times (10, 20, 30 min). Each condition was performed in technical triplicate, totalizing 27 samples. After adding 500 µL mixture of water type I:MeOH (3:1 v/v), the samples were vortexed and centrifuged for 5 min at 4 ºC, 10000 rpm (Mikro 220R, Andreas Hettich GmbH & Corporation, Tuttlingen, Germany). The three phases were separated and dried in a vacuum concentrator (Concentrator Plus, Eppendorf AG, Hamburg, Germany), at ambient temperature under vacuum-alcoholic mode, and stored at –80 ºC until the chromatographic analysis. The workflow is presented in Figure 1 and the experimental design is presented in Table 1.

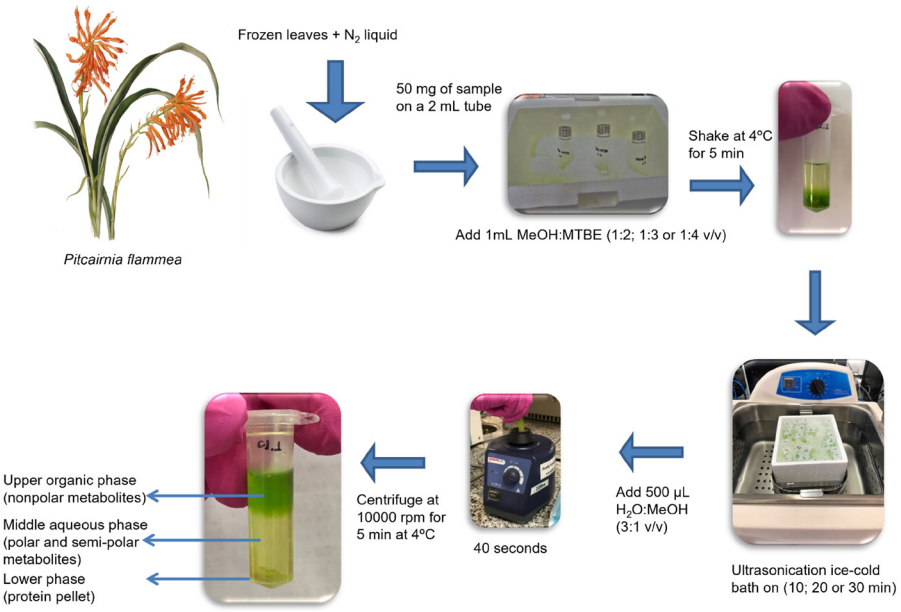

Figure 1. Flowchart of extraction steps from leaves of *Pitcairnia flammea.*

Table 1. Experimental design of the extraction with solvent proportion and time of ultrasonic bath

Group	time / min	A 10	B 20	C 30
	Proportion			
1	1:2	A1.1, A1.2, A1.3	B1.1, B1.2, B1.3	C1.1, C1.2, C1.3
2	1:3	A2.1, A2.2, A2.3	B2.1, B2.2, B2.3	C2.1, C2.2, C2.3
3	1:4	A3.1, A3.2, A3.3	B3.1, B3.2, B3.3	C3.1, C3.2, C3.3

Liquid chromatography coupled to mass spectrometry analysis

The upper phase (lipid or organic phase) was re-suspended in a mixture of solvents corresponding to the initial of the chromatographic run: 60% mobile phase A and 40% mobile phase B. Mobile phase A was composed of acetonitrile:water (40:60, v/v) and mobile phase B was acetonitrile:2-propanol (10:90, v/v). In both chromatographic mobile phases, 10 mmol L^{-1} NH_4Ac was added. Quality control (QC) samples were prepared using 5 µL of each filtered extract to a vial with a 150 µL insert. One vial with acetonitrile was used as system suitability blank sample for further checks on impurities and instrumental fluctuations. Reversed-phase liquid chromatography was performed in an UHPLC system (UltiMate™ 3000 RSLCnano system, Thermo Scientific, Waltham, USA) using a Titan C_{18} column with 100 mm × 2.1 mm × 1.9 µm particle size (Supelco Sigma-Aldrich, Bellefonte, USA). The sample injection volume was set to 5 µL and the column and sampler temperature were kept at 40 and 10 ºC, respectively. Separation was performed at a 250 µL min^{-1} flow rate under a gradient elution mode. Over the next 2 min, the column was re-equilibrated before the next injection. The total execution time was 14 min (Table 2).

Table 2. Gradient of solvents at chromatographic separation

time of analysis / min	Mobile phase	
	A / %	B / %
0-2	60	40
2-3	50	50
3-6	50	50
6.1	30	70
6.1-8	30	70
8-9	0	100
9-11	0	100
11-12	60	40
12-14	60	40

Detection was performed using a Orbitrap Q-Exactive (Thermo Scientific, Waltham, USA) mass spectrometer equipped with a heated-ESI source operating on the positive and negative ionization modes using the MS full scan followed by MS/MS analysis in the data-dependent acquisition mode of the 5 most intense peaks. Full scan data were acquired between *m/z* 100 and 1500 in profile mode and at resolution 70000 (at *m/z* = 200). The automatic gain control was set as automatic gain control target at 1×10^6, 1 scan s^{-1}, and injection time at 100 ms. Heated-ESI parameters were optimized for both ionization modes, as follows: sheath gas flow rate 35 arbitrary units; auxiliary gas flow rate 10 arbitrary units; and capillary temperature

300 °C. For the spray voltage, the positive ion mode was +3.5 kV, and the negative ion mode was −3.2 kV. The ion optics setting was S-Lens RF level 50; S-Lens 25 V; skimmer 15 V; and C-Trap RF 1010 V. Stepped normalized collision energy was 20-30-40.

Data analysis

Manual extraction of UHPLC-ESI-MS chromatograms, signal intensity, and total ion detection were achieved using Thermo Xcalibur Roadmap 3.1 from the raw data. For pre-processing data on MS-DIAL 4.9 software,[14] UHPLC-ESI-MS raw data were converted to .mzML extension on MSConverter 3.0 from ProteoWizard.[15,16] The parameter analysis were setting with MS^1 tolerance of 0.02 Da, MS^2 tolerance 0.06 Da, retention time 0-14 min, MS^1 and MS^2 *m/z* 100-1500 range, maximum charged number 1; peak detection with 10000 of minimum peak height and mass slice width of 0.1 Da; deconvolution with MS/MS abundance cut off of 30 amplitude and sigma window value of 0.5; alignment parameters with retention time tolerance 0.5 min, MS^1 tolerance of 0.02 Da and removed features based on blank information.[17] For identification, the default of accurate mass tolerance was used as 0.01 Da for MS^1 and 0.05 Da for MS^2, and identification score cut off 80%. Adduct forms selected were $[M - H]^-$, $[M - H_2O - H]^-$, $[M + Na - 2H]^-$, and $[M + Cl]^-$ for negative ionization mode, and $[M + H]^+$, $[M + NH_4]^+$, $[M + Na]^+$, and $[M + CH_3OH + H]^+$ for the positive one. The peak spot viewer was filtered to show just the peaks matched according to the reference libraries and with MS/MS information (Figure S1, Supplementary Information (SI) section). MS-DIAL internal lipid annotation is based on LipidBlast.[18]

The aligned MS-DIAL results (.csv file) were exported using raw data matrix (area; 28 columns (+ and −), 19803 rows (+), 29092 rows (−)) filtered by the ion abundance of blank sample containing retention time, *m/z* and intensity of each feature with sample and group name, used for pre-treatment and statistical analyses on MetaboAnalyst 5.0.[19] For this step, first, positive ionization data variables were normalized by sum and then a 30% relative standard deviation (RSD) threshold and cube root transformation and auto scaling were performed. For negative ionization data, the normalization by QC sample, 30% RSD, log transformation and Pareto scaling were performed. Multivariate analysis (principal component analysis (PCA), hierarchical clustering analysis (HCA) (distance measure: Euclidean; clustering algorithm: Ward)), and univariate analysis (Volcano plot (fold change threshold: 2.0, *p*-adjusted value by false discovery rate threshold: 0.05)) were performed.

The lipidomics datasets of this article were deposited and processed at Metabolomics Workbench,[20] with the identifier PR001657 (study ID ST002570).[21]

Results and Discussion

Chromatographic analysis

An originally used Bligh and Dyer[22] extraction method has been modified, enhancing lipid extraction procedures from plant material.[22-24] Among these modifications, the MTBE substitution not only was environmentally friendly, but also improved the reproducibility during aliquoting, since the organic phase became the upper layer.[3,25] Three-phase extraction methods have gained prominence in plant studies, since the interference of polar metabolites was reduced by optimizing the phase separation in the lipid analysis.[26,27] To this preliminary evaluation of the extraction parameters, the method performed by Hummel *et al*.[13] for a lipid comprehensive profile of leaves was used as a basis, since it is a simple, fast, and one-step protocol.

Samples that were extracted using the lowest solvent proportion (MeOH:MTBE 1:2, v/v) and lowest time on ultrasonic ice-cold bath (10 and 20 min) did not present separation phases after centrifugation (Figure S2a, SI section). On the other hand, in samples extracted using MeOH:MTBE 1:2 (v/v) at 30 min on ultrasonic in ice-cold bath, the formation of the three separation phases was verified (Figure S2b, SI section). This separation was also verified in samples extracted with MeOH:MTBE at the 1:3 and 1:4 (v/v) proportions. Homogenization procedure is a crucial step in sample preparation to guarantee a successful extraction, even more in plants, which have rigid tissues. Axelsson and Gentili[24] compared two microwave conditions, Potter-Elvehjelm homogenizer, sonication and no treatment for microalgae cell disruption and did not observe a total lipid yield gain. However, in this study, the time was essential for lipid extractability on MeOH:MTBE 1:2 (v/v) solvent system.

Besides the extraction method, the separation method has great impact on the untargeted analysis of complex lipidome samples.[28] In terms of chromatography, the optimized method for lipids already used for human samples[29] was also satisfactory for plant material (Figure S3, SI section). Reversed-phase liquid chromatography using acetonitrile, H_2O and isopropanol as mobile phase is one of the most applied strategies in plant lipidomic studies, being liquid chromatography coupled to mass spectrometry a highly efficient technique to analyze complex isomeric samples as lipids in plant tissues.[3] It is noteworthy that the use of gradient mobile phase with isopropanol results

in higher noise signals in high retention times mainly in negative ionization mode (Figure S3a, SI section). This behavior is also presented by Criscuolo *et al*.[30] comparing C_{18} and C_{30} columns.

Semiquantitative results

To analyze the influence of the experimental parameters and their contribution to the lipid profile, data on the number of signal intensities and number of total ions detected were compiled and presented in Tables 3 and 4, respectively. These tables were used to compare the values obtained from the different parameter combinations.

Signal intensities were utilized to assess the amount of potential individual compounds that could be detected in the samples, without the influence of the base peak. On the other hand, the number of total ions detected was used to evaluate which parameter combination would extract more information from the samples. The analysis was based on the total ion chromatogram, which is a chromatogram obtained by summing up the intensities of all the mass spectral peaks belonging to the same scan.

In order to analyze the influence of the extraction method employed, the mean signal intensities for the entire chromatographic run of each sample and groups were compiled in Table 3. The positive ionization mode

Table 3. Signal intensities for the entire chromatographic run based on the analysis of the base peak chromatograms

Solvent ratio	No.	Signal intensities / a.u.					
		Group A (+) ($\times 10^9$)	Group A (–) ($\times 10^8$)	Group B (+) ($\times 10^9$)	Group B (–) ($\times 10^8$)	Group C (+) ($\times 10^9$)	Group C (–) ($\times 10^8$)
1:2	1	–	–	–	–	2.41	4.93
	2	–	–	–	–	2.59	4.59
	3	–	–	–	–	2.69	4.62
$\bar{x} \pm s$		–	–	–	–	2.5 ± 0.1	4.7 ± 0.2
1:3	1	3.15	5.88	2.61	6.60	3.21	5.44
	2	2.44	7.27	2.40	5.15	2.70	4.82
	3	3.39	5.52	2.66	5.26	2.90	5.24
$\bar{x} \pm s$		3.0 ± 0.5	6.2 ± 0.9	2.6 ± 0.1	5.7 ± 0.8	2.9 ± 0.3	5.2 ± 0.3
1:4	1	3.72	7.56	2.73	5.25	2.60	4.74
	2	2.73	5.46	2.66	5.22	2.56	4.91
	3	2.16	5.03	2.87	5.96	3.18	5.41
$\bar{x} \pm s$		2.9 ± 0.8	6 ± 1	2.8 ± 0.1	5.5 ± 0.4	2.8 ± 0.4	5.0 ± 0.4

No.: replicates; (+): positive mode; (–): negative mode. Group A: samples submitted to 10 min of ultrasonic bath; Group B: samples submitted to 20 min of ultrasonic bath; Group C: samples submitted to 30 min of ultrasonic bath. Groups A and B extracted in a 1:2 ratio of solvent did not present phase separation and, therefore, were not subjected to chromatographic analysis; a.u.: arbitrary units; $\bar{x} \pm s$: mean ± standard deviation.

Table 4. Number of total detected ions in each sample and mean of extraction condition groups

Solvent ratio	Total detected ions						
	No.	Group A (+)	Group A (–)	Group B (+)	Group B (–)	Group C (+)	Group C (–)
1:2	1	–	–	–	–	31289	35074
	2	–	–	–	–	31534	34962
	3	–	–	–	–	31177	34958
$\bar{x}$		–	–	–	–	31333	34998
1:3	1	31215	35546	31241	35127	31399	34937
	2	31327	35125	31133	34947	31162	35185
	3	31592	35243	31537	35186	31674	34906
$\bar{x}$		31378	35304	31303	35086	31411	35009
1:4	1	31228	35310	30979	35121	30929	35117
	2	30888	34999	31046	35242	31115	35180
	3	30994	35373	31316	34744	31595	34988
$\bar{x}$		31036	35227	31113	35035	31213	35095

No.: replicates; (+): positive mode; (–): negative mode. Group A, B and C: samples submitted to 10, 20 and 30 min of ultrasonic bath, respectively. Groups A and B extracted in a 1:2 ratio of solvent did not present phase separation, for this reason, they were not subjected to chromatographic analysis. $\bar{x}$: mean.

presented a greater magnitude order than the negative one. Samples extracted with MeOH:MTBE 1:3 (v/v) for 10 min at ultrasonic ice-cold bath presented highest average intensities in both ionization modes (2.99×10^9 (+) and 6.22×10^8(–)).

The number of detected ions were compiled in Table 4, to optimize the visualization regarding the influence of the ionization mode and extraction process for lipid analysis in plant. It was observed that the negative mode displayed a higher number of detected ions than the positive mode. In addition, samples extracted with solvent proportion MeOH:MTBE 1:3 (v/v) exhibited highest mean of detected ions: 31411 for positive mode in 30 min and 35304 for negative mode in 10 min ultrasonic ice-cold bath.

Statistical analysis

By conducting an analysis of aligned data on MS-DIAL,[31] it is possible to achieve an overview of lipid classes distribution in *m/z versus* retention time in both ionization modes along the peak spot viewer (Figure S1, SI section). In this study, 311 compounds were putatively identified on negative ionization mode, while in the positive mode, 274 compounds were identified based on MS/MS information. Besides the known lipid distribution based on compound size along the chromatographic run,[2,13] we also can access lipid subclasses for each ionization mode. In studies that intend to analyze specific lipid subclasses, such as phosphatidylcholines or ceramides, data obtained on positive ionization mode would be more suitable. On the other hand, if phosphatidic acids or sterols are the focus on answer a specific biological question, a better option would be performing analyses in the negative ionization mode. Cajka and Fiehn[28] presented a table in their review with different molecular species formed by lipid subclasses in both ionization modes and pointed out that despite the positive mode is more used in lipidomics, some lipids as phosphatidylinositol are favored in the negative ionization mode. Therefore, the use of both ionization modes provides complementary information such as the alteration of fatty acids due to oxidative stress and increased triacylglycerol levels due to heat stress, for example.[6]

From the positive and negative ionization modes, 42 chromatograms were acquired from experimental samples plus QC and solvent blank samples by using UHPLC-ESI-MS. The sequence setup started with one blank, followed by 5 QCs, three of those for system conditioning, followed by another blank and then, the experimental samples. The QC data used to conditioning the platform were not used for data processing, since this data is more variable than the ones used intra-batch.[31] The samples were randomly organized in batches to avoid bias and the use of blank samples is recommended to assess the system suitability.[32,33] Furthermore, one QC sample was analyzed after every 10 experimental samples. A manual analysis of this amount of data could lead to erroneous data interpretation; therefore, MetaboAnalyst 5.0 was the free platform employed to pre-treat and to perform statistical analysis, allowing the user to choose the one that better fits the data.[34] In the context of metabolomics/lipidomics analysis, a predefined pre-treatment data protocol is lacking. Following multiple attempts at applying transformation and normalization techniques, the data distribution was observed to assume a Gaussian shape, which is presented in Figure S4 (SI section) as the most optimal outcome.

The unsupervised statistical analysis, PCA, was applied to all samples to evaluate the instrumental stability and trends between sample groups. PCA scores plot (Figure S5, SI section) presents that most of QC samples in the negative ionization mode are clustered, indicating a satisfactory method.[32] However, QC4-NEG, and QC5-NEG diverge from the other QC samples. UHPLC-ESI-MS analyses were performed first on positive mode then on negative mode. The QC sample was the same for both ionization modes. QC-NEG 4 and 5 were analyzed at the end of positive and the beginning of the negative ionization mode analyses indicating a concentration variation in these anomalous samples (Figure S6, SI section). Subsequently, these anomalous data were removed from the matrix data to follow the statistical analysis (Figure 2a). In the positive ionization mode, most of the QC data are clustered (Figure 2c).

Referring to the sample extraction, most of the samples overlap (Figures 2a, 2c). However, inspecting the samples that were obtained under 30 min of ultrasonic ice-bath (group C), we can see a trend to distribute the samples group along the PC1 on negative mode (Figure 2a) and on PC2 for positive mode (Figure 2c). This behavior is confirmed by HCA. HCA is a strategy that builds a hierarchy of clusters ordering the samples according to their similarity. HCA dendrogram presents a similarity between C2 and C3 groups, which was not observed between C1 and them (Figure 2b), indicating the influence of the solvent proportion on the sample lipid composition. The same trend is observed on PCA scores plot and HCA dendrogram of positive ionization mode data (Figures 2c, 2d).

Following this, to enhance our comprehension of the influence of solvent proportion on the sample lipid composition, a Volcano plot was built using the extreme groups of solvent proportion (Figure S7, SI section). According to MetaboAnalyst, "Volcano plot combines results from fold change (FC) analysis and *t*-tests into

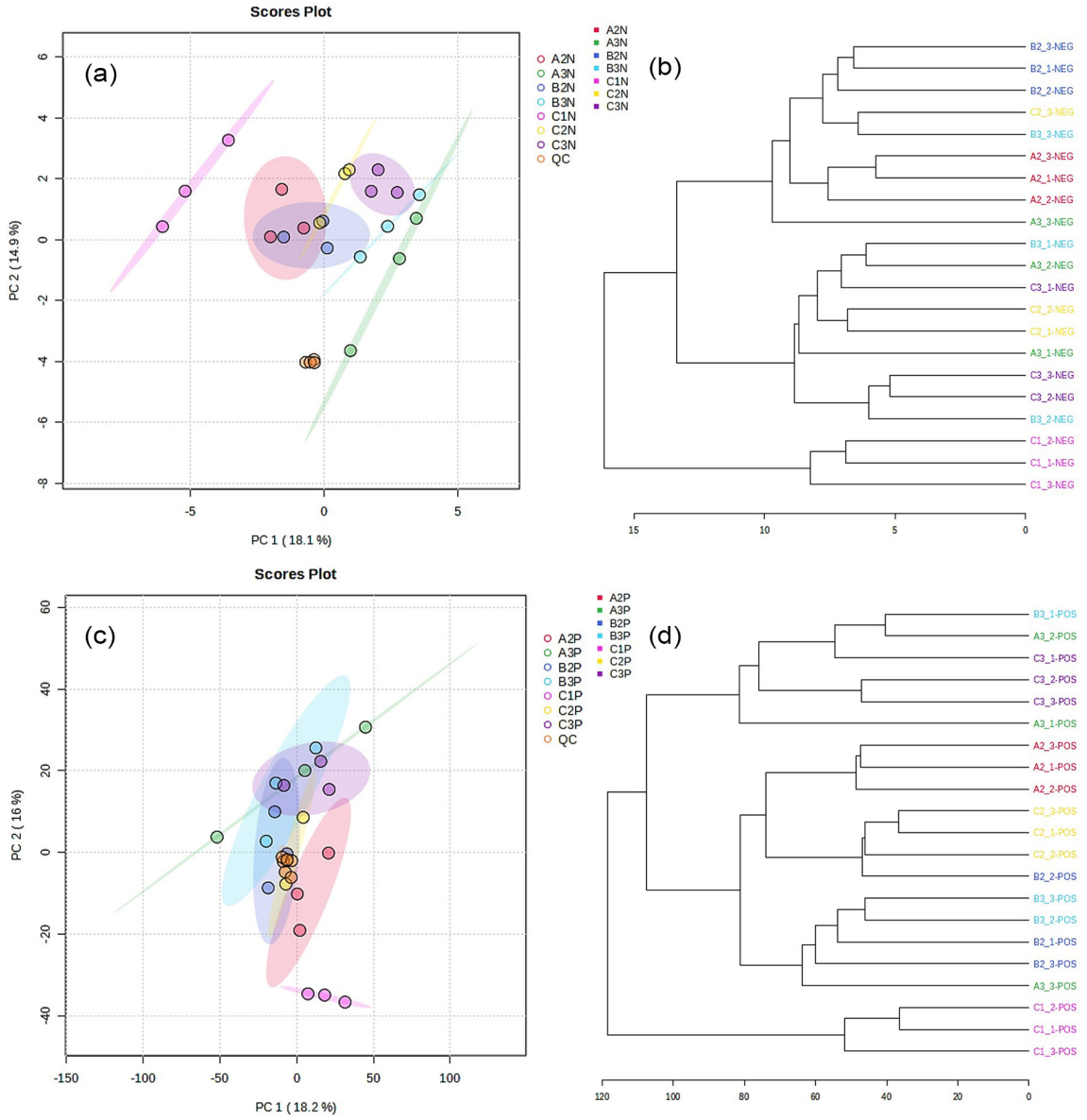

Figure 2. Unsupervised methods varying the extraction parameters. (a) PCA scores plot based on negative ionization mode. (b) HCA dendrogram of samples analyzed in negative ionization mode. (c) PCA scores plot based on positive ionization mode. (d) HCA dendrogram of samples analyzed on positive ionization mode. Samples named A, B, and C: time in ultrasonic bath for 10, 20, or 30 min, respectively. 1, 2, and 3: solvent ratio (v/v) at 1:2, 1:3, and 1:4, respectively.

one single graph which allows users to intuitively select significant features based on either biological significance, statistical significance, or both".[20] The comparison direction of Volcano plot was 1/3, that is, smallest solvent ratio to largest one.

Among the features detected in both ionization modes as significative to group discrimination, only six compounds were putatively identified by MS-DIAL internal library (Table 5). All the features statistically relevant to the comparisons are presented in the SI section (Tables S1 and S2). Table 5 displays that only one fatty acid was identified as decreased in the samples extracted in the smallest solvent ratio, 1:2 (v/v), compared to the highest one, 1:4 (v/v). In light of this, if this lipid class was object of interest, it is suggested that MeOH:MTBE 1:4 (v/v) is the best option as solvent mixture for extraction, besides the negative ionization mode application. With the obtained results, no lipid subclass was suggested as favored using the smallest solvent ratio of MeOH:MTBE 1:2 (v/v). Moreover, no compound was identified among the significant, in the positive ionization mode data using the solvent ratio parameter.

Back to Figure 2, it is not possible to observe any trend to separate or cluster based on the time in ultrasonic bath. However, the Volcano plot allows to select statistically significant variables to the 10 × 30 min

Table 5. Putative identification of differential compounds from the comparisons analyzed in both ionization modes with p-value < 0.05

Parameter	t_R / min	*m/z*	Log_2 (FC)	Level	*p*-value	Adduct	Description[35]
Ratio 1 × 3	0.885	329.2338	−10.16	↓	2.21×10^{-3}	$[M - H]^-$	FA 18:1;3O
time A × C	4.026	518.3253	15.71	↑	6.22×10^{-3}	$[M + H]^+$	LPC 18:3
time A × C	5.088	520.3417	15.52	↑	1.53×10^{-2}	$[M + H]^+$	LPC 18:2
time A × C	10.908	629.5119	−15.57	↓	2.09×10^{-2}	$[M + Na]^+$	DG 35:2
time A × C	10.660	608.5262	−15.59	↓	3.99×10^{-2}	$[M + NH_4]^+$	DG 34:3
time A × C	10.893	612.5579	−6.65	↓	4.24×10^{-2}	$[M + NH_4]^+$	DG 34:1

FC: fold change. Samples group named 1 and 3: solvent ratio (v/v) at 1:2, and 1:4, respectively. Samples group named A and C: time in ultrasonic bath for 10, and 30 min, respectively. FA: fatty acid. LPC: lysophophatidylcholine. DG: diacylglycerol. ↓: lower abundance and ↑: higher abundance.

comparison suggesting some lipid subclasses (Figure S8, SI section). As can be seen in Table 5, if diacylglycerol or/and lysophosphatidylcholine is the focus of the study, the positive ionization mode analysis would bring more information. Nevertheless, diacylglycerol could be favored in higher extraction time, while lysophosphatidylcholine could be enriched in the 10 min ultrasonic ice bath method. For the time parameter, any feature of the 15 (Table S2) was identified in the negative ionization mode.

The combination of solvent ratio and time in ultrasonic bath had more influence on sample composition indicated by the sample trend (group C) than just to evaluate one parameter. These parameters have a great impact on the extraction as demonstrated by Chua *et al*.[36] in 2009, where in an optimization of ultrasound usage for palm-pressed fiber, time was considered a relevant variable in the extraction of phosphatidylethanolamine, phosphatidylcholine and total lipids.

The use of styrofoam box during the ultrasonic bath is an aspect that could affect the result of extraction and can be mitigated with the use of cold water or ice on the bath increasing the extraction efficiency, since higher ultrasonic exposure times yield higher peak intensities, although at higher temperatures this effect is reduced.[37] One limitation of this study still is a metabolomics/lipidomics bottleneck: the annotation. At the same time, many features were detected as statistically significant (Tables S1 and S2), but a few were annotated. In the plant kingdom, at least 250 sterols and 400 fatty acids were identified, for example.[38] Perhaps, the use of more than one library could be complementary and enhance the identification number. As a result, more information could be obtained from lipid subclasses variations related to the extraction parameters. Additionally, the cultivation condition can influence the results since bromeliads have a high adaptative ability.[39] As lipids have major roles in response to abiotic stress,[6,40] some subclasses could have been favored by sampling. However, the application of statistical tools and use of the same sample varying just the extraction condition method can mitigate that and give some clues in a targeted analysis.

The results presented in this work can bring insights into several metabolic pathways in plant biology. For instance, phosphatidylmethanol, ceramides and diacylglycerol have been indicated as biomarkers of cold stress in *Bryum pseudotriquetrum* and *Psyscomitrium patens*,[41] as well as in storage lipid conversion and extreme condition signaling in alfalfa leaves.[42] Therefore, future targeted or class-focused lipidomics of said lipids can be greatly improved by solvent and time related changes in sample preparation.

Regarding time-related variations of the lipidome, in positive ionization mode, lysophosphatidylcholine compounds are the most prominent lipid classes. This class of lipids is important to monitor specially in food storing processes, since *trans*-fatty acids are harmful to human health, and they are a direct degradation product of glycerolipids and glycerophospholipids.[43]

Conclusions

The untargeted lipidomic analyses of complex samples as a plant extract have many steps that can be optimized to enhance the results. Sample preparation comparison studies can help researchers to choose the best methodology for their issue. UHPLC-ESI-MS in combination with bioinformatics platforms have been increasingly and widely used bringing to light information that was previously confusing and/or obscured by conventional analysis techniques. In this paper, we evaluated the influence of sample preparation parameters and electrospray ionization mode selection on the lipid composition results in a plant model. By employing chemometrics methods, we could not suggest any difference in lipid classes based on the variation of extraction solvent proportion in the positive ionization mode. However, in the negative ionization mode, there was a decrease of fatty acid compounds identified using a lower solvent proportion. Considering the 30 min ultrasonic ice bath extraction method, there was variation in the

lysophosphatidylcholine and diacylglycerol composition in the positive ionization mode. Consequently, we highlight the importance of optimization of the sample preparation methods, especially if the focus is on a particular lipid class as a target or in a global lipidomics study.

Supplementary Information

Supplementary data are available free of charge at http://jbcs.sbq.org.br as PDF file.

Acknowledgments

Coordenação de Aperfeiçoamento de Pessoal de Nível Superior (CAPES) grant number: 88887.372951/2019-00; Conselho Nacional de Desenvolvimento Científico e Tecnológico (CNPq) grant numbers: 131700/2022-7 and 306662/2022-1, and INCT of Bioanalytics (FAPESP 2014/50867-3 and CNPq 465389/2014-7 grant numbers) are acknowledged for financial support. We thank the LaBIOmics group for professional and friendly support, especially Luidy Darllan Barbosa and Thales Fernando Dias Pereira for programming and Bruna Beatriz Soldera for experimental assistance. The authors also thank Diego Campaci de Andrade for technical assistance.

Author Contributions

Taynara S. Matos was responsible for conceptualization, data curation, formal analysis, investigation, methodology, validation, visualization, and writing-original draft; Mariana S. Marques and Flávia S. Zandonadi for formal analysis, and writing-original draft; Cleber J. N. Chaves and Clarisse Palma-Silva for investigation, resources, and writing-review and editing; Alessandra Sussulini for conceptualization, funding acquisition, project administration, resources, supervision, and writing-review and editing.

References

1. Fiehn, O.; *Comp. Funct. Genomics* **2001**, *2*, 155. [Crossref]
2. Lange, M.; Ni, Z.; Criscuolo, A.; Fedorova, M.; *Chromatographia* **2019**, *82*, 77. [Crossref]
3. Kehelpannala, C.; Rupasinghe, T.; Hennessy, T.; Bradley, D.; Ebert, B.; Roessner, U.; *Mol. Omics* **2021**, *17*, 894. [Crossref]
4. Brown, H. A.; Marnett, L. J.; *Chem. Rev.* **2011**, *111*, 5817. [Crossref]
5. Liu, N.-J.; Wang, N.; Bao, J.-J.; Zhu, H.-X.; Wang, L.-J.; Chen, X.-Y.; *Mol. Plant* **2020**, *13*, 1523. [Crossref]
6. He, M.; Ding, N. Z.; *Front. Plant Sci.* **2020**, *11*, 562785. [Crossref]
7. Nemati, M.; Singh, B.; Mir, R. A.; Nemati, M.; Babaei, A.; Ahmadi, M.; Rasmi, Y.; Golezani, A. G.; Rezaie, J.; *Cell Commun. Signal.* **2022**, *20*, 69. [Crossref]
8. Britt, H. M.; Cragnolini, T.; Khatun, S.; Hatimy, A.; James, J.; Page, N.; Williams, J. P.; Hughes, C.; Denny, R.; Thalassinos, K.; Vissers, J. P. C.; *Rapid Commun. Mass Spectrom.* **2022**, *36*, e9308. [Crossref]
9. Zeki, Ö. C.; Eylem, C. C.; Reçber, T.; Kır, S.; Nemutlu, E.; *J. Pharm. Biomed. Anal.* **2020**, *190*, 113509. [Crossref]
10. Bi, H.; Guo, Z.; Jia, X.; Liu, H.; Ma, L.; Xue, L.; *Metabolomics* **2020**, *16*, 68. [Crossref]
11. Gika, H.; Theodoridis, G.; *Bioanalysis* **2011**, *3*, 1647. [Crossref]
12. Sun, F.; Chen, H.; Chen, D.; Tan, H.; Huang, Y.; Cozzolino, D.; *J. Agric. Food Chem.* **2020**, *68*, 11309. [Crossref]
13. Hummel, J.; Segu, S.; Li, Y.; Irgang, S.; Jueppner, J.; Giavalisco, P.; *Front. Plant Sci.* **2011**, *2*, 54. [Crossref]
14. MS-DIAL, http://prime.psc.riken.jp/compms/msdial/main.html, accessed in May 2023.
15. Chambers, M. C.; Maclean, B.; Burke, R.; Amodei, D.; Ruderman, D. L.; Neumann, S.; Gatto, L.; Fischer, B.; Pratt, B.; Egertson, J.; Hoff, K.; Kessner, D.; Tasman, N.; Shulman, N.; Frewen, B.; Baker, T. A.; Brusniak, M.-Y.; Paulse, C.; Creasy, D.; Flashner, L.; Kani, K.; Moulding, C.; Seymour, S. L.; Nuwaysir, L. M.; Lefebvre, B.; Kuhlmann, F.; Roark, J.; Rainer, P.; Detlev, S.; Hemenway, T.; Huhmer, A.; Langridge, J.; Connolly, B.; Chadick, T.; Holly, K.; Eckels, J.; Deutsch, E. W.; Moritz, R. L.; Katz, J. E.; Agus, D. B.; MacCoss, M.; Tabb, D. L.; Mallick, P.; *Nat. Biotechnol.* **2012**, *30*, 918. [Crossref]
16. Proteowizard, https://proteowizard.sourceforge.io/download.html, accessed in May 2023.
17. Zandonadi, F. S.; Silva, A. A. R.; Melo, A. A. S.; Ignarro, R. S.; Matos, T. S.; Santos, E. A. F.; Barbosa, L. D.; Oliveira, A. L. R.; Porcari, A. M.; Sussulini, A.; *Anal. Bioanal. Chem.* **2023**, *415*, 4367. [Crossref]
18. Kind, T.; Liu, K.-H.; Lee, D. Y.; DeFelice, B.; Meissen, J. K.; Fiehn, O.; *Nat. Methods* **2013**, *10*, 755. [Crossref]
19. MetaboAnalyst 5.0, https://www.metaboanalyst.ca/, accessed in May 2023.
20. Sud, M.; Fahy, E.; Cotter, D.; Azam, K.; Vadivelu, I.; Burant, C.; Edison, A.; Fiehn, O.; Higashi, R.; Nair, K. S.; Sumner, S.; Subramaniam, S.; *Nucleic Acids Res.* **2016**, *44*, D463. [Crossref]
21. Summary of project PR001657, https://www.metabolomicsworkbench.org/data/DRCCMetadata.php?Mode=Project&ProjectID=PR001657, accessed in May 2023.
22. Bligh, E. G.; Dyer, W. J.; *Can. J. Biochem. Physiol.* **1959**, *37*, 911. [Crossref]
23. Kehelpannala, C.; Rupasinghe, T. W. T.; Hennessy, T.; Bradley, D.; Ebert, B.; Roessner, U.; *Plant Methods* **2020**, *16*, 155. [Crossref]
24. Axelsson, M.; Gentili, F.; *PLoS One* **2014**, *9*, e89643. [Crossref]
25. Coman, C.; Solari, F. A.; Hentschel, A.; Sickmann, A.; Zahedi, R. P.; Ahrends, R.; *Mol. Cell. Proteomics* **2016**, *15*, 1453. [Crossref]

26. Shiva, S.; Enninful, R.; Roth, M. R.; Tamura, P.; Jagadish, K.; Welti, R.; *Plant Methods* **2018**, *14*, 14. [Crossref]
27. Kang, J.; David, L.; Li, Y.; Cang, J.; Chen, S.; *Front. Genet.* **2021**, *12*, 635971. [Crossref]
28. Cajka, T.; Fiehn, O.; *TrAC, Trends Anal. Chem.* **2014**, *61*, 192. [Crossref]
29. Ribeiro, H. C.; Klassen, A.; Pedrini, M.; Carvalho, M. S.; Rizzo, L. B.; Noto, M. N.; Zeni-Graiff, M.; Sethi, S.; Fonseca, F. A. H.; Tasic, L.; Hayashi, M. A. F.; Cordeiro, Q.; Brietzke, E.; Sussulini, A.; *Psychiatry Res.* **2017**, *258*, 268. [Crossref]
30. Criscuolo, A.; Zeller, M.; Cook, K.; Angelidou, G.; Fedorova, M.; *Chem. Phys. Lipids* **2019**, *221*, 120. [Crossref]
31. Tsugawa, H.; Cajka, T.; Kind, T.; Ma, Y.; Higgins, B.; Ikeda, K.; Kanazawa, M.; Vandergheynst, J.; Fiehn, O.; Arita, M.; *Nat. Methods* **2015**, *12*, 523. [Crossref]
32. Broadhurst, D.; Goodacre, R.; Reinke, S. N.; Kuligowski, J.; Wilson, I. D.; Lewis, M. R.; Dunn, W. B.; *Metabolomics* **2018**, *14*, 72. [Crossref]
33. Kirwan, J. A.; Gika, H.; Beger, R. D.; Bearden, D.; Dunn, W. B.; Goodacre, R.; Theodoridis, G.; Witting, M.; Yu, L.-R.; Wilson, I. D.; *Metabolomics* **2022**, *18*, 70. [Crossref]
34. Chong, J.; Wishart, D. S.; Xia, J.; *Curr. Protoc. Bioinforma.* **2019**, *68*, 1. [Crossref]
35. Liebisch, G.; Fahy, E.; Aoki, J.; Dennis, E. A.; Durand, T.; Ejsing, C. S.; Fedorova, M.; Feussner, I.; Griffiths, W. J.; Köfeler, H.; Merrill, A. H.; Murphy, R. C.; O'Donnell, V. B.; Oskolkova, O.; Subramaniam, S.; Wakelam, M. J. O.; Spener, F.; *J. Lipid Res.* **2020**, *61*, 1539. [Crossref]
36. Chua, S. C.; Tan, C. P.; Mirhosseini, H.; Lai, O. M.; Long, K.; Baharin, B. S.; *J. Food Eng.* **2009**, *92*, 403. [Crossref]
37. Klein-Júnior, L. C.; Viaene, J.; Salton, J.; Koetz, M.; Gasper, A. L.; Henriques, A. T.; Vander Heyden, Y.; *J. Chromatogr. A* **2016**, *1463*, 60. [Crossref]
38. Reszczyńska, E.; Hanaka, A.; *Cell Biochem. Biophys.* **2020**, *78*, 401. [Crossref]
39. Palma-Silva, C.; Leal, B. S. S.; Chaves, C. J. N.; Fay, M. F.; *Bot. J. Linn. Soc.* **2016**, *181*, 305. [Crossref]
40. Shiva, S.; Samarakoon, T.; Lowe, K. A.; Roach, C.; Vu, H. S.; Colter, M.; Porras, H.; Hwang, C.; Roth, M. R.; Tamura, P.; Li, M.; Schrick, K.; Shah, J.; Wang, X.; Wang, H.; Welti, R.; *Plants* **2020**, *9*, 845. [Crossref]
41. Lu, Y.; Eiriksson, F. F.; Thorsteinsdóttir, M.; Simonsen, H. T.; *Plant-Environment Interact.* **2022**, *3*, 254. [Crossref]
42. Li, M.; Yu, A.; Sun, Y.; Hu, Q.; Kang, J.; Chen, L.; Zhu, X.; Yang, Q.; Long, R.; *Environ. Exp. Bot.* **2023**, *205*, 105144. [Crossref]
43. Jia, X.; Yang, X.; Xu, M.; Tan, W.; Yin, M.; Liu, P.; Tong, H.; *Postharvest Biol. Technol.* **2023**, *199*, 112297. [Crossref]

Submitted: March 21, 2023
Published online: June 6, 2023